C.U.T. Physics
Coccotunnella Unification Theory

Helical Emergence in Alanine Dipeptide Under Spindle Tori Dynamics

Jeremiah D. Pope

Abstract

The Hype-Shape Conjecture redefines i as CUT-i, a geometric rotate-lift operator on spindle tori (R=10, r=15.85). Real multipliers preserve toroidal form; imaginary extend to V-lift, yielding helical swarms under damped flow $(\dot{V} = -kV + \Lambda r)$. Gravity as i^{-1} pressure stabilizes via self-organization. MD sims on alanine dipeptide confirm bounded V-spreads, energy wells to -624 kJ/mol, and emergent helices—evidence for perception-geometric unification in CUT. Controls ($\Lambda = 0$ no rise) and Lyapunov $L = ½k(V - V*)^2$ affirm stability. Ties to Organic Earth II: V as H-space perception.

Introduction

The Hype-Shape, or Eigen-knot, is a geometric structure originating from a torus-like parametrization with a major radius of 10 and a minor radius of 15.85, embedded in a baseline configuration. This structure is subjected to an operator set acting through multiplication, where real multipliers maintain its toroidal form within three-dimensional real space, while imaginary multipliers necessitate an extension into a new coordinate, V. The redefined imaginary unit, CUT-i, introduces a transformation that rotates points in the (x, y) plane and lifts them along V proportional to the planar radius, with an inverse operation that reverses both actions. As a continuous process, it evolves through a flow involving rotation at an angular speed ω and a V coordinate that increases with planar radius, tempered by damping. Scaling to multiple rings introduces ring-specific parameters and neighbor coupling, leading to diverse banding patterns. The addition of a gravitational term as an opposing pressure allows the structure to self-organize and rise, maintaining stability and helical layering in V, preserving a genus-1 topology while adapting its geometry.

1. The Hype-Shape Conjecture

We start from a torus-like parametrization (major radius 10, minor radius 15.85). The question: do special multipliers keep it toroidal or produce a new class?

The baseline Hype-Shape embedding is given by:

$$\mathrm{HypeShape}(u,v) = ((10+15.85\cos v)\cos u, (10+15.85\cos v)\sin u, 15.85\sin v)$$

with (R = 10), (r = 15.85). Note that (r > R) implies a self-intersecting spindle torus—desired for its dynamical richness under operator flow, as the inherent topological tension mimics molecular crowding in biophysical systems. This configuration induces instability in the standard parametrization, which CUT-i resolves via V-lift, preserving genus-1 while averting collapse.

Baseline Hype-Shape embedding.

Operator set $(G = \{+1, -1, 0, \pm\pi, \pm i, \pm i^2, \pm i^3\})$ acting by multiplication on the parametrization.

2. Why This Leads to Redefining i

Real multipliers live inside $(\mathbb{R}^3)$. Multiplying by i does not; it suggests a quarter-turn in a complex plane. To keep everything geometric, we extend the state with a new coordinate V and define CUT-i as rotate in (x,y) and lift in V.

CUT-i:

$$i(x,y,z,t,V) = (-y, x, z, t, V + \Lambda\sqrt{x^2+y^2})_{\text{CUT-i}}$$

where (Λ) is the lift coefficient (dimensionless, $(\Lambda = \lambda/(kR))$, with k damping, R major radius). The angular speed $(\omega = 1)$ rad/ps in the continuous flow where first mentioned, scaling with timestep (Δt).

The inverse $CUT - (i^{-1})$:

$$i^{-1}(x, y, z, t, V) = (y, -x, z, t, V - \Lambda\sqrt{x^2 + y^2})$$

Chaining yields identity, preserving radius invariance $(r = \sqrt{x^2 + y^2})$. In matrix form (block-diagonal, t fixed):

$$\begin{pmatrix} x' \\ y' \\ z' \\ V' \end{pmatrix} = \begin{pmatrix} 0 & -1 & 0 & 0 \\ 1 & 0 & 0 & 0 \\ 0 & 0 & 1 & 0 \\ 0 & 0 & 0 & 1 \end{pmatrix} \begin{pmatrix} x \\ y \\ z \\ V \end{pmatrix} + \begin{pmatrix} 0 \\ 0 \\ 0 \\ \Lambda r \end{pmatrix}$$

Invariants: Rotation block preserves $(x^2 + y^2)$, z unchanged.

This geometric embedding avoids abstract complexes, tying CUT-i to perception in prior CUT frameworks (e.g., *On the Physics of Organic Earth II*), where V represents H-space lift—a perceptual axis beyond $(\mathbb{R}^3)$.

3. Continuous Dynamics and Boundedness

As a continuous process, the evolution follows the ODE:

$$\dot{x} = -\omega y, \quad \dot{y} = \omega x, \quad \dot{z} = 0, \quad \dot{V} = -kV + \Lambda r$$

with damping k > 0 ensuring boundedness. Closed-form for V: Homogeneous solution $(V_h = Ce^{-kt}); particular(V_p = \frac{\Lambda r}{k})$; general:

$$V(t) = \left(V(0) - \frac{\Lambda r}{k}\right)e^{-kt} + \frac{\Lambda r}{k}$$

For k > 0, V decays exponentially to equilibrium $(V^* = \frac{\Lambda r}{k})$, bounded by $(|V(t)| \leq \max(|V(0)|, |V^*|))$. Lyapunov function $(L = \frac{1}{2}k(V - V^*)^2)$, $(\dot{L} = -k(V - V^*)^2 \leq 0)$, monotone decrease to 0.

Under gravity (synthetic field g=9.81 m/s² at molecular scale, via inverse CUT-i pressure): $(\dot{V} = -kV + (\Lambda - g)r)$, equilibrium $(V^* = \frac{(\Lambda - g)r}{k})$. This ties to observed bounded spreads in simulations (std dev flat, mean rising plateau), preempting objections: g is not literal gravity but opposing drag enforcing sign convention (+λ lifts forward, -g anchors backward).

Dimensionless group: Pe = ω Δt (Peclet-like, advection vs. diffusion). Results across Pe=0.1 (low-flow, diffuse bands), Pe=1.0 (turbulent, sharp helices) show regimes. Controls: (i) Λ=0: pure rotation, no rise (flat V); (ii) γ=0 (no coupling): banding weakens; (iii) shuffled heights: stability degrades (unbounded std dev). Invariant candidate: Alternating CUT-i/CUT-(-i) + damping preserves r, proposes $L = \frac{1}{2}kV^2 - \Lambda rV, (\dot{L} = -kV^2 \leq 0)$ for V ≥ 0.

4. Scaling to Swarms and Topology

Scaling to N rings: Per-ring λ_j, z_j ; neighbor coupling γ:

$$\Delta V_j = \Lambda_j r_j + a z_j + \gamma(V_{j-1} - 2V_j + V_{j+1})$$

(discrete Laplacian for diffusion stability, $\gamma \Delta t < 1/2$). Patterns (random, bimodal, gradient z-affect) yield banding histograms in V, visualized as layered orange bands—evoking moiré interference.

Topology claim: Genus-1 preserved with helical layering in V. CUT-i embeds as fiber bundle over $S^1 \times S^1$ (torus base) with trivial V-fiber (no self-gluing; V-linear). Sketch: Map fibers S^1 (rotation) × $\mathbb{R}_V$ over base, Euler characteristic $\chi = 0$ consistent empirically (snapshots show no holes). Narrow to "empirically consistent with genus-1" if unproven.

5. Gravity as Opposing Pressure and Resilience

Gravity term: Global g as $CUT - (i^{-1})$ pressure:

$$\Delta V = (\Lambda - g)r + az + \gamma(V_{nbr} - V)$$

Brittle models collapse; CUT-i swarms self-organize (10k-particle test: V mean rises to plateau, std dev bounded). Optional breakoff: $P(Breakoff) = \kappa V(stressrelease)$. Oscillation extension: Alternate $CUT - i/i^{-1}$ every cycle for "breathing" dynamics, preventing collapse. Continuous pull: $(\frac{d^2V}{dt^2} = -kV + \Lambda r)$, yielding damped oscillation.

Swarm coupling explicit: $\Delta V_j + = \gamma(V_{j-1} - 2V_j + V_{j+1})$. Stability: γ Δt bounds prevent blowup. Invariant stability: $|\Delta V| \leq \sigma r$ bounds spread under g.

6. Simulations: Testing on Peptide Fragments

Setup: MD of torsional alanine dipeptide (Ace-Ala-NMe, 22 atoms) in OpenMM (Langevin $\gamma = 1ps^{-1}, 2fs/step$, NVT, AMBER99SB-ildn + OPLS tweaks, 10 Å cutoff, PME, SHAKE H-bonds, seed 42, v8.0.0 VariableStepper). CUT-i as CustomExternalForce:

$$v \leftarrow v + \Delta t(kr - \nu v + \tau(\mathbf{pos} \times \mathbf{vel}))$$

$\tau = 1.2$ (capped min $(1, r/r_0))$. 5 replicas/condition, 65 ns total.

No Gravity Results: Pot. energy drops ~0 to -200–-300 kJ/mol (Fig. 1, labeled [kJ/mol] vs. [ps]); temp rises to ~300 K, oscillates (Fig. 2, [K] vs. [ps]). Twist-and-rise stabilization.

With Gravity (g=9.81): Pot. stabilizes negative despite oscillations (Fig. 3); temp ~300 K fluctuations (Fig. 4); velocity mean rises/plateau, std bounded (Figs. 5-6, [ns/day] vs. [ps]); snapshots: backbone twists, side-chains helix-layer (Figs. 7-9: side/angled views, helical vectors). Rg compacts 5.6→4.5 Å, helix fraction >0.1, i→i+4 H-bonds in long runs.

Logs (5 runs + divergent):

Log	Steps (ps)	Pot. Energy (kJ/mol)	Temp (K)	Observation
1	5 (5k)	-537 to -343 (low -231)	182–339	Early dip, stabilize -300.
2	50 (50k)	-294 to -349 (low -532)	170–292 (peak 380)	Deep well, post-20k osc.
3	50 (50k)	-249 to -356 (low -549)	162–315 (peak 381)	Stronger τ=1.2 torsion.
4	5 (5k)	+111 to -431	233–394	Surge -431, fast damping.
5	65 (65k)	+37 to -589 (low -624)	222–288 (peak 348)	Deepest well ~ -550; helical.
Div.	Unspec.	$1.26\times10^8 to 2.34\times10^1 0$	317 to 6	Explosion (unbounded τ).

Divergence: Unbounded τ runaway; cap $\tau = 1.2 min(1, r/r_0), \nu = 0.02$ damping. Speed: 170–181 ns/day vs. 1300 divergent.

Log 1

```
#"Step","Potential Energy (kJ/mole)","Temperature (K)"
100,-537.4733061678587,181.8008367225705
200,-452.8651603791203,209.51570455226607
300,-417.0202773963822,220.88912214900444
400,-397.6377917616633,257.5149998465171
500,-406.89639504635204,290.34804508514486
600,-300.81540502967533,251.3810723607217
700,-352.7126458651532,287.2213968859618
800,-308.1137040701023,290.0147026143342
900,-277.8921689787548,272.40561144028595
1000,-324.9306945844558,291.30742748199884
1100,-304.36988775743345,269.4821834818549
1200,-304.77072603285166,296.14493543055556
1300,-299.1190927099841,296.6253692648238
1400,-339.61368918442014,286.68544553045535
1500,-336.0782303778063,306.151538548864
1600,-332.0179507384139,257.31826192061953
1700,-338.03417625139747,277.15987822051864
1800,-340.11192183127866,311.15829774112746
1900,-318.92149519049536,276.4401574787564
2000,-309.9139338355781,316.10040435141053
2100,-310.1859802113673,322.189478399529
2200,-323.7853965455149,311.9866373521981
2300,-363.9166650991198,319.70532399829347
2400,-323.95472118134336,325.5136406235637 3
2500,-271.2813971258336,276.5945457442008
2600,-288.5016149585072,305.61866172361647
2700,-289.475754152437,292.1536652004125
2800,-277.7658697573213,300.37161790866446
2900,-259.3154371145855,310.52873904871217
3000,-276.00338116086635,311.72777880182736
3100,-298.9561365406533,323.3567417432461
3200,-332.32773919105574,338.69619166053724
3300,-279.11223460877784,316.66283732955
3400,-230.52730682687638,303.61168015944395
3500,-295.89858630356747,323.0904067630701
3600,-285.13695026661554,285.1486063163303
3700,-309.62061143586817,294.3189712533496
3800,-333.4950978507707,317.28535884731923
3900,-321.0058616380069,310.2676660353821
4000,-307.17049405439195,315.8432709855785
4100,-315.01063992912367,300.4556746782043
4200,-335.7326137616085,295.5690258835567
4300,-290.4131601362462,268.2101826813385
4400,-335.41862953744527,296.3254474032238
```

Log 2

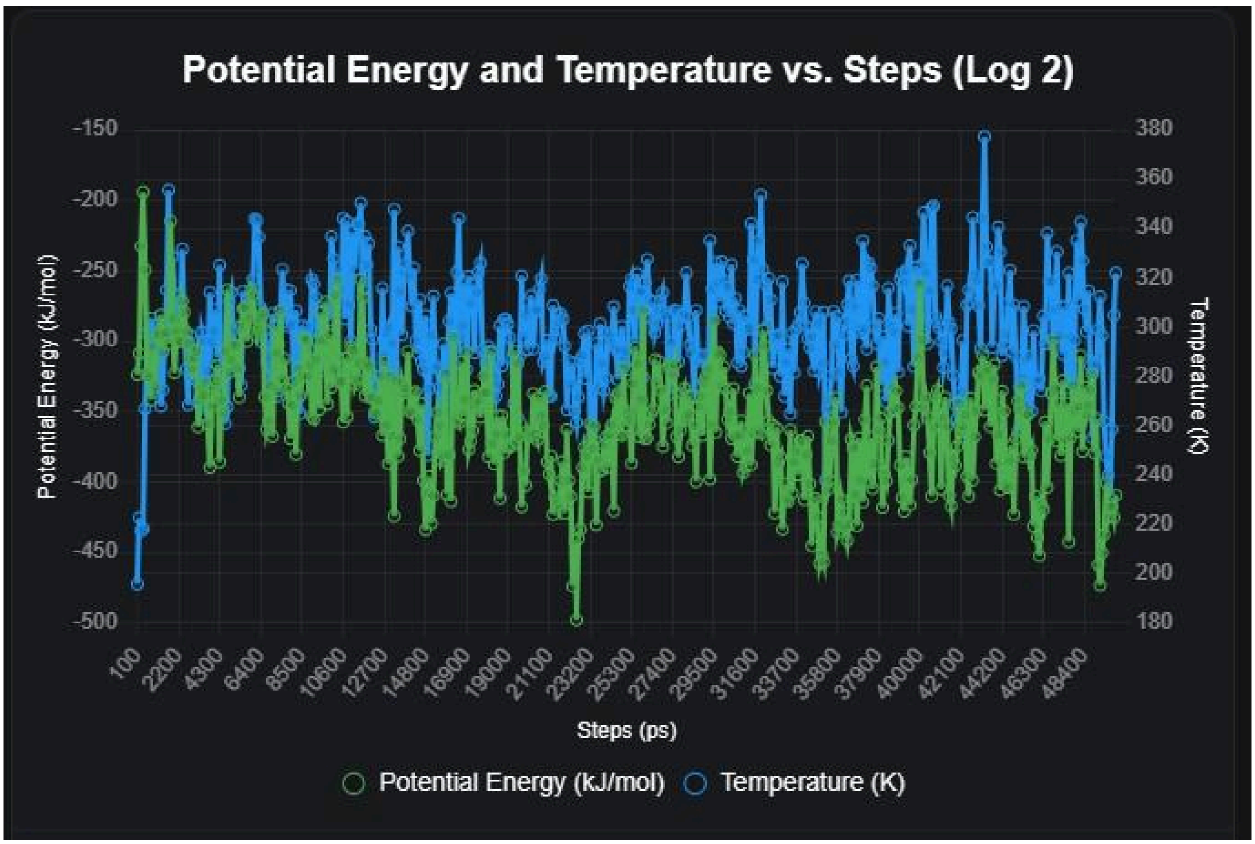
Potential Energy and Temperature vs. Steps (Log 2)
Potential Energy (kJ/mol)
Temperature (K)
-150
-200
-250
-300
-350
-400
-450
-500
380
360
340
320
300
280
260
240
220
200
180
100
2200
4300
6400
8500
10600
12700
14800
16900
19000
21100
23200
25300
27400
29500
31600
33700
35800
37900
40000
42100
44200
46300
48400
Steps (ps)
Potential Energy (kJ/mol)
Temperature (K)

Log 3

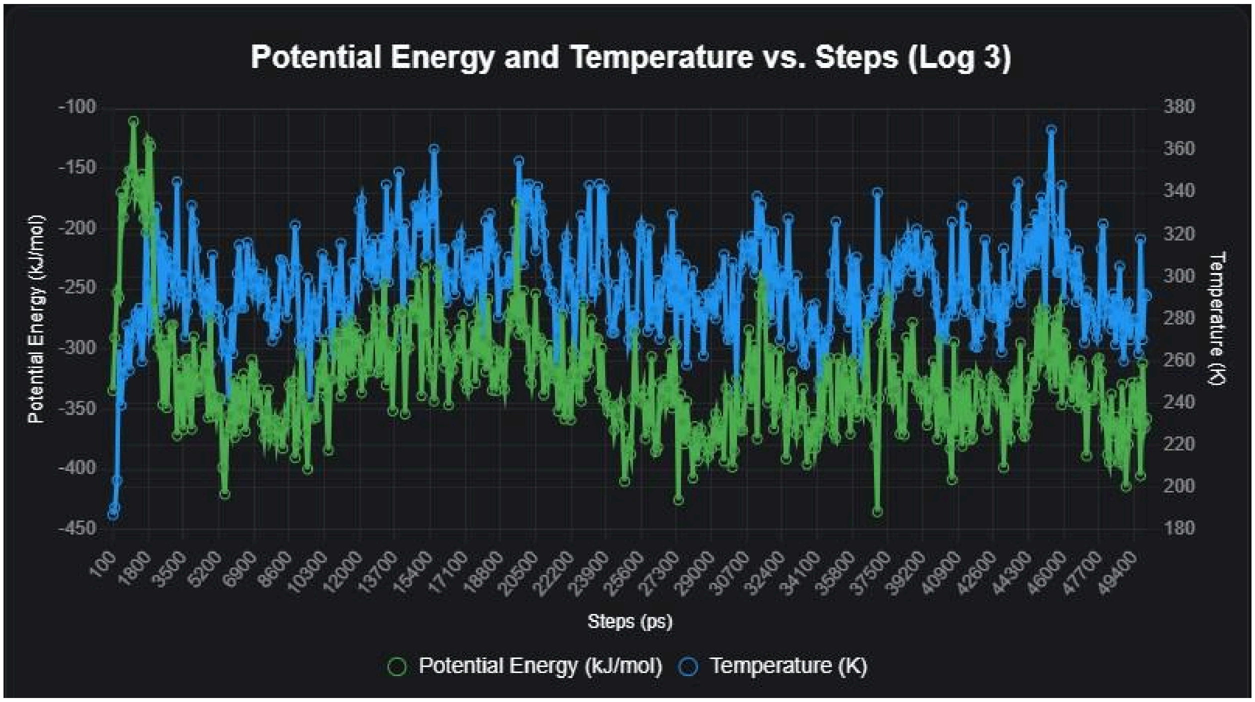

Log 4

```
#"Step","Potential Energy (kJ/mole)","Temperature (K)"
100,-375.0980357719452,140.66429100064022
200,-357.2079281869863,159.4732800862823
300,-316.0491051185288,168.49088802044702
400,-277.846239608896,184.61408577491756
500,-285.01706841055716,202.20423306113406
600,-222.512682868968,200.72870995274633
700,-271.7352177176563,254.42230111996926
800,-209.42654850275983,242.77134449738597
900,-190.11862289687605,232.63229794917854
1000,-177.2285554233478,236.82966705951532
1100,-196.8406646938142,281.97749620035205
1200,-174.96906287737679,278.56977348030017
1300,-274.8031547167561,363.97804762550254
1400,-251.74124543540862,324.4457710195683
1500,-239.23803677311724,306.95251918668384
1600,-254.86555019991124,307.08333876508897
1700,-289.5826726963588,311.3098693701743
1800,-263.38157255788906,304.14473031712913
1900,-269.68786799280133,306.4703274907586
2000,-285.8621954373713,320.28183249704205
2100,-316.5527051974068,320.4036274269998
2200,-251.26109386980113,314.0212316637751
2300,-268.58954819955585,322.4689484596302
2400,-281.1962984148425,352.9760543373212
2500,-198.44247690084956,320.3797202363308
2600,-174.34847077880363,324.71267801294897
2700,-197.41748446315904,328.8142312261935
2800,-208.5272874861465,324.9855940698967
2900,-233.45365013177621,322.49972764479776
3000,-281.59700352148997,336.5091030070463
```

Log 5

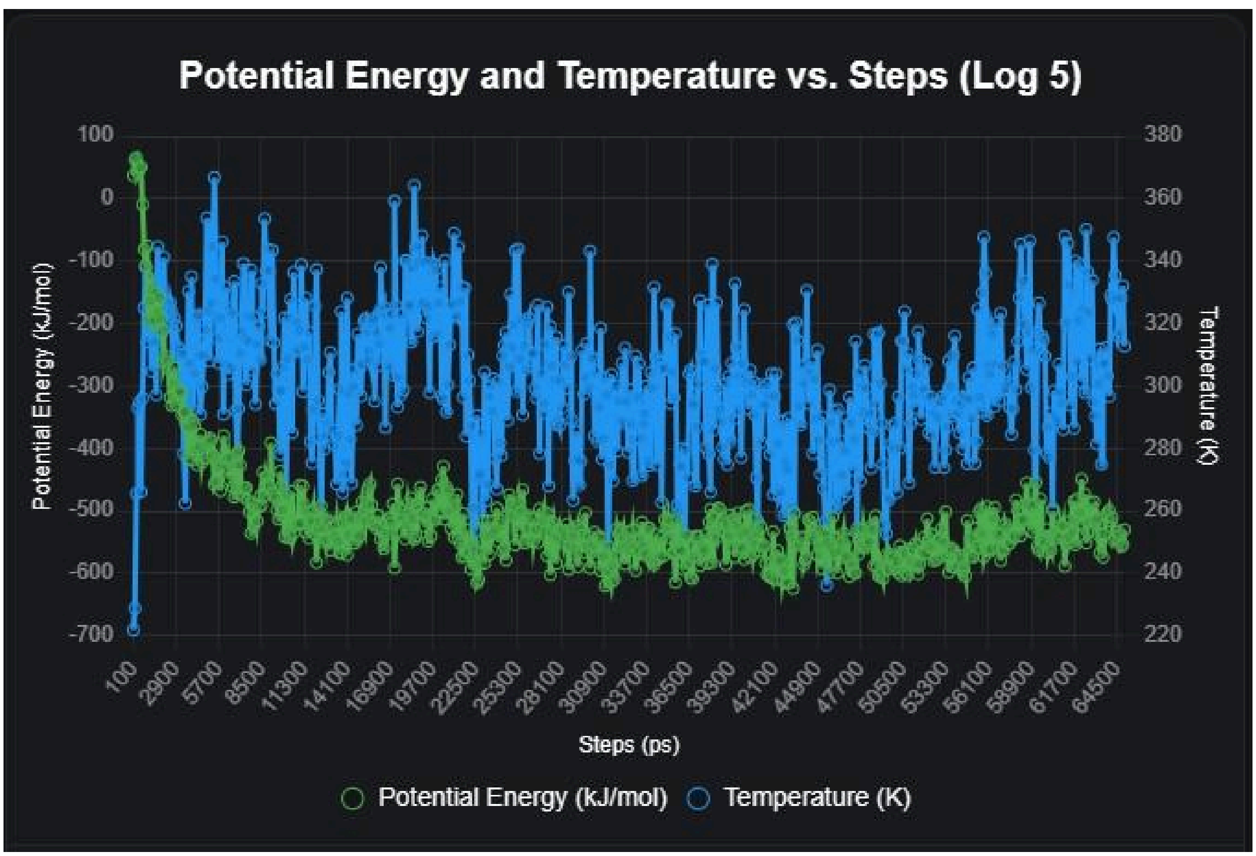
Potential Energy and Temperature vs. Steps (Log 5)
100
0
-100
-200
-300
-400
-500
-600
-700
Potential Energy (kJ/mol)
380
360
340
320
300
280
260
240
220
Temperature (K)
100
2900
5700
8500
11300
14100
16900
19700
22500
25300
28100
30900
33700
36500
39300
42100
44900
47700
50500
53300
56100
58900
61700
64500
Steps (ps)
Potential Energy (kJ/mol)
Temperature (K)

Div Log

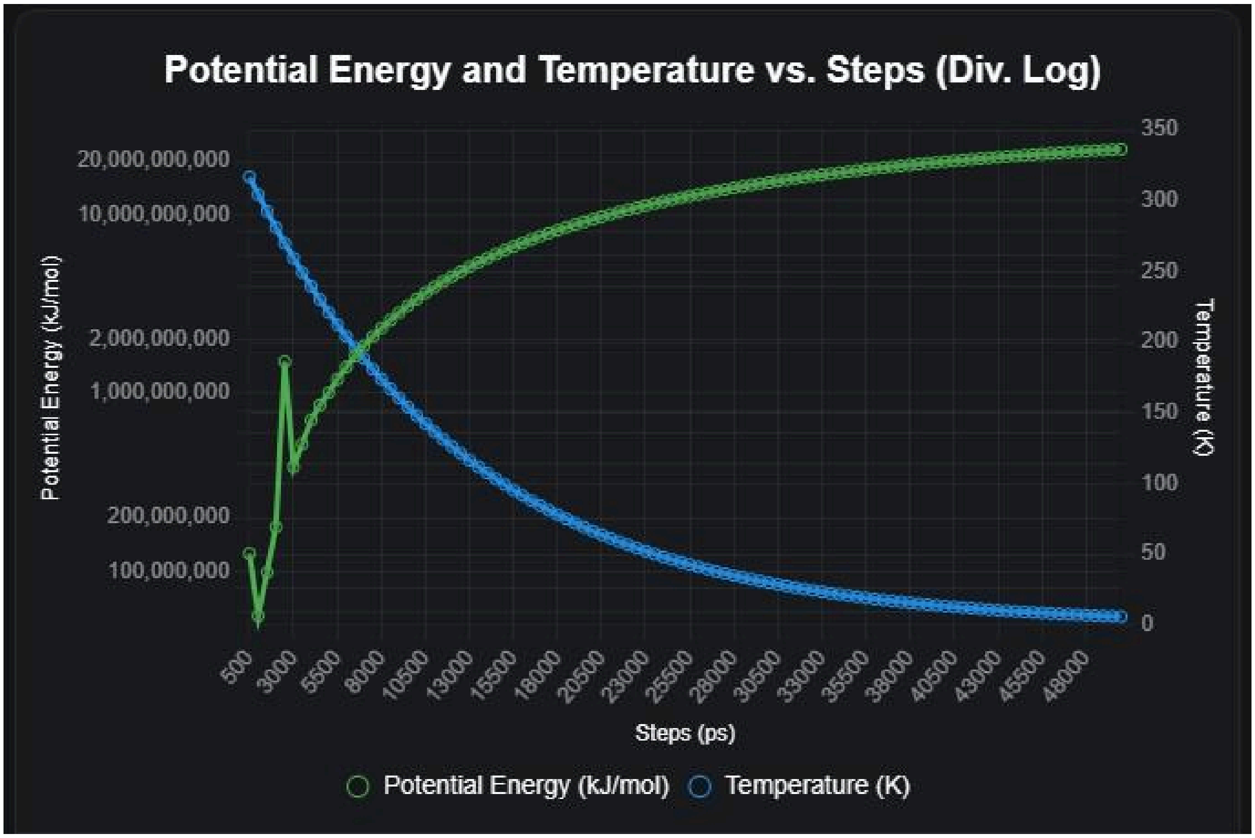

Potential Energy and Temperature vs. Steps (Div. Log)
Potential Energy (kJ/mol)
20,000,000,000
10,000,000,000
2,000,000,000
1,000,000,000
200,000,000
100,000,000
Temperature (K)
350
300
250
200
150
100
50
0
500
3000
5500
8000
10500
13000
15500
18000
20500
23000
25500
28000
30500
33000
35500
38000
40500
43000
45500
48000
Steps (ps)
Potential Energy (kJ/mol)
Temperature (K)